Transverse gradient diffusion in a polydisperse dilute suspension of magnetic spheres during sedimentation

2008 J. Phys.: Condens. Matter 20 204129

(http://iopscience.iop.org/0953-8984/20/20/204129)

IOP Publishing Journal of Physics: Condensed Matter

J. Phys.: Condens. Matter **20** (2008) 204129 (5pp) doi:10.1088/0953-8984/20/20/204129

Transverse gradient diffusion in a polydisperse dilute suspension of magnetic spheres during sedimentation

F R Cunha and H L G Couto

Departamento de Engenharia Mecânica, Universidade de Brasília, Faculdade de Tecnologia, Grupo de Mecânica dos Fluidos de Escoamentos Complexos—VORTEX, Campus Universitário Darcy Ribeiro, 70910-900, Brasília, DF, Brazil

E-mail: frcunha@unb.br

Received 3 April 2008
Published 1 May 2008
Online at stacks.iop.org/JPhysCM/20/204129

Abstract

In this work we investigate the pair interaction of magnetic particles in a dilute polydisperse sedimenting suspension. The suspension is composed of magnetic spherical forms of different radii and densities immersed in a Newtonian fluid, settling due to the gravity. When in close contact, the particles may exert on each other a magnetic force due to a permanent magnetization. We restrict our attention to dispersions of micromagnetic composite with negligible Brownian motion. The calculations of the relative particle trajectories are based on direct computations of the hydrodynamic interactions among rigid spheres in the regime of low particle Reynolds number. Depending on the relative importance of the interparticle forces and gravity, the collisions may result in aggregation or simply in a breaking of the particle relative trajectory time reversibility. After summing over all possible encounters, the transverse self-diffusion and down-gradient diffusion coefficients that describe the cross-flow migration of the particles are calculated. Our calculation shows first evidence and the significance of the diffusion process arising from magnetic interactions in dilute non-Brownian suspensions.

1. Introduction

In a dilute dispersion, the probability of a third sphere influencing the relative motion of two interacting particles is small, and so we only need to consider binary interactions of particles. If Brownian motion, inertia and interparticle forces are negligible, two spherical particles collide in a sedimenting dilute suspension in a reversible way, returning to their initial streamlines. However, when the interparticle forces are significant the particles are subjected to a lateral migration and hence the collisions may result in aggregation or simply in a breaking of the time reversibility of the particle relative trajectory.

The migration of non-colloidal particles in a suspension gives rise to a dispersive process which may be characterized as self-dispersion owing to the random nature of collisions among the suspended particles. The first experimental investigations were carried out by Eckstein *et al* [1], who determined the lateral shear-induced coefficient of self-dispersion of spherical particles in a Couette device. A pioneering work [2] considered the interactions between two rigid conducting spheres under shear flow, evaluating the influence of a long-range force over the lateral particle migration. In addition, Wang *et al* [3, 4] presented expressions for the shear-induced self-diffusivity and gradient diffusivity of a tracer fluid particle and of a test sphere in the two directions perpendicular to the fluid velocity, and Cunha and Hinch [5] presented results for the transverse shear-induced gradient diffusivity for simple shearing of a dilute suspension of rough spheres. Their theory was applied to study self-dispersion of deformable drops, using a boundary integral scheme [6]. For sedimenting suspensions, the hydrodynamic diffusivity has been determined for a rough heavy sphere and/or smooth sphere falling through a dilute suspension of neutrally buoyant spheres [7, 8]. Self-diffusion in more concentrated suspensions of non-Brownian particles in simple shear flow has been studied using accelerated Stokesian dynamics simulation [9, 10].

This paper presents a theoretical calculation of the relative trajectories of two interacting magnetic particles in a dilute sedimenting suspension. We should point out that in the

current literature there is no well-established general theory on this problem to which we can appeal. On the basis of the previous results [5], we derived a general expression for the transverse self-diffusion and gradient-diffusion coefficients for a polydisperse dilute suspension. These calculations are independent of the flow and the nature of the force between the particles. Here we take into account the influence of particle magnetization on breaking the relative trajectory time reversibility coming from a trajectory analysis for different conditions of the parameters which considers the relative importance of interparticle forces and gravity.

2. Statement of the problem

Consider a bidisperse dilute suspension of rigid smooth magnetic spheres of radius a_1 and a_2, densities ρ_1 and ρ_2 and magnetizations $\boldsymbol{M}_1 = M_1\hat{\boldsymbol{d}}_1$ and $\boldsymbol{M}_2 = M_2\hat{\boldsymbol{d}}_2$ immersed in a Newtonian fluid of density ρ and viscosity μ. Furthermore, the particle Reynolds number is assumed to be vanishingly small, so that all inertia effects can be ignored and the creeping flow equations can be applied on the scale of the particle motion. We suppose that the particles are not sufficiently massive so that their inertia need not be included when determining their trajectories. We shall restrict our attention in this first calculation to dilute dispersions in which the induced torque on the test particle due to the permanent magnetization of the second particle is a weak effect. The suspension undergoes a uniform gravitational force per unit mass $\boldsymbol{g} = -g\hat{\boldsymbol{e}}_2$.

The pairwise collisions of the particles in non-Brownian suspensions are gravity induced due to the different particle radii and densities. The polydispersity of the pair of particles is characterized by the radius ratio $\lambda \equiv (a_2/a_1)$ and by the reduced densities ratio $\gamma \equiv (\rho_2 - \rho)/(\rho_1 - \rho)$. The centres of the particles 1 and 2 are located at $\boldsymbol{X}$ and $\boldsymbol{Y}$, respectively, where $\boldsymbol{r} \equiv \boldsymbol{Y} - \boldsymbol{X} = r\,\hat{\boldsymbol{r}}$ denotes the vector joining the centres of the two particles, and the dimensionless distance between the particles is denoted by $s \equiv 2r/(a_1 + a_2)$. The settling velocity of an isolated particle of the species i is given by $\boldsymbol{U}_i^{(0)} = 2\,a_i^2(\rho_i - \rho)\,\boldsymbol{g}/9\mu$. The relative velocity of the isolated particles is defined as being $\boldsymbol{U}_{12}^{(0)} \equiv \boldsymbol{U}_2^{(0)} - \boldsymbol{U}_1^{(0)}$, and its absolute value $U_{12}^{(0)}$ will be used in the present context as a velocity scale of the motion.

3. Mobility formulation

As the creeping flow equations are linear and quasi-steady, the velocity of each sphere depends only on the instantaneous relative location of the two spheres, and is linear with respect to the applied forces, $\boldsymbol{F}_1$ and $\boldsymbol{F}_2$. Thus, the translational velocities $\boldsymbol{U}_1$ and $\boldsymbol{U}_2$ are determined by the following mobility relations [11]:

$$\boldsymbol{U}_1 = \boldsymbol{b}_{11}\boldsymbol{F}_1 + \boldsymbol{b}_{12}\boldsymbol{F}_2 \qquad \text{and} \qquad \boldsymbol{U}_2 = \boldsymbol{b}_{21}\boldsymbol{F}_1 + \boldsymbol{b}_{22}\boldsymbol{F}_2 \quad (1)$$

with $b_{\alpha\beta} = [3\pi\mu(a_\alpha + a_\beta)]^{-1}[\mathcal{A}_{\alpha\beta}(\boldsymbol{rr}/r^2) + \mathcal{B}_{\alpha\beta}(\boldsymbol{I} - (\boldsymbol{rr}/r^2))]$, where the square matrix is the global mobility, that contains the second-order tensors $\boldsymbol{b}_{\alpha\beta}(\alpha, \beta = 1, 2)$ and $\boldsymbol{I}$ denotes the unit second-order tensor. The two-sphere mobility functions $\mathcal{A}_{\alpha\beta}(s, \lambda)$ and $\mathcal{B}_{\alpha\beta}(s, \lambda)$ depend only on λ and the dimensionless distance s. Numerical values of the mobility functions for arbitrary λ and s have been made available by [12, 11] for the near-field and far-field configurations. Acting on the particles, the $\boldsymbol{F}_i$ force includes the buoyancy force and the magnetic interaction force, being expressed as $\boldsymbol{F}_i = \frac{4}{3}\pi a_i^3(\rho_i - \rho)\boldsymbol{g} + (2i - 3)\nabla\varphi_{\mathrm{M}}$ for $i = 1, 2$, where φ_{M} is the magnetic potential.

3.1. Magnetic pairwise interaction

For the magnetic interaction between two dipoles, the far-field expression given in [13] applies: $\varphi_{\mathrm{M}} = [\mu_0(M_1V_1)(M_2V_2)]/(4\pi r^3)[\hat{\boldsymbol{d}}_1 \cdot \hat{\boldsymbol{d}}_2 - 3(\hat{\boldsymbol{d}}_1 \cdot \hat{\boldsymbol{r}})(\hat{\boldsymbol{d}}_2 \cdot \hat{\boldsymbol{r}})]$, where $\hat{\boldsymbol{r}} \equiv \boldsymbol{r}/r$ is the unit vector along the line of centres of the particles, V_1 and V_2 are the particle volumes and μ_0 is the magnetic permeability of the free space. For the non-dimensioning of this equation, we chose as a typical scale $\mu_0 M_1^2 V_1$, being a measure of the strength of the magnetic potential. Then, it can be rewritten in a dimensionless form as $\varphi_{\mathrm{M}}^{\mathrm{d}} = (M_{12}/(3\,s^3))(2\lambda/(1+\lambda))^3[\hat{\boldsymbol{d}}_1 \cdot \hat{\boldsymbol{d}}_2 - 3(\hat{\boldsymbol{d}}_1 \cdot \hat{\boldsymbol{s}})(\hat{\boldsymbol{d}}_2 \cdot \hat{\boldsymbol{s}})]$, where $M_{12} = M_2/M_1$ is the magnetization intensity ratio and $\varphi_{\mathrm{M}}^{\mathrm{d}} = \varphi_{\mathrm{M}}/\mu_0 M_1^2 V_1$.

3.2. Particle relative trajectory

The equation of the motion of the two spheres consists in the balance between the hydrodynamic force on each particle and the applied force $\boldsymbol{F}_i$. Thus, the vector $\boldsymbol{s}$ time evolution, in a dimensionless form, is governed by the differential equation $\mathrm{d}\boldsymbol{s}/\mathrm{d}t = \boldsymbol{U}_{12} \equiv \boldsymbol{U}_2 - \boldsymbol{U}_1$. And, by substituting the expression for $\boldsymbol{F}_i$ into (1), one obtains an expression for the relative velocity $\boldsymbol{U}_{12}$ given by

$$\boldsymbol{U}_{12} = \boldsymbol{e}_2 \cdot \left[\frac{\boldsymbol{ss}}{s^2}\mathcal{L} + \left(\boldsymbol{I} - \frac{\boldsymbol{ss}}{s^2}\right)\mathcal{M}\right] - \mathcal{Q}_{\mathrm{M}}\nabla\varphi_{\mathrm{M}}^{\mathrm{d}} \cdot \left[\frac{\boldsymbol{ss}}{s^2}\mathcal{G} + \left(\boldsymbol{I} - \frac{\boldsymbol{ss}}{s^2}\right)\mathcal{H}\right] \quad (2)$$

where $\mathcal{L}$, $\mathcal{M}$, $\mathcal{G}$ and $\mathcal{H}$ are scalar functions of s [12, 11] given by $\mathcal{L}(s) = \frac{\gamma\lambda^2 A_{22} - A_{11}}{\gamma\lambda^2 - 1} + \frac{2(1-\gamma\lambda^3)A_{12}}{(\gamma\lambda^2-1)(1+\lambda)}$, $\mathcal{M}(s) = \frac{\gamma\lambda^2 B_{22} - B_{11}}{\gamma\lambda^2 - 1} + \frac{2(1-\gamma\lambda^3)B_{12}}{(\gamma\lambda^2-1)(1+\lambda)}$, $\mathcal{G}(s) = \frac{\lambda A_{11} + A_{22}}{(1+\lambda)} - \frac{4\lambda A_{12}}{(1+\lambda)^2}$ and $\mathcal{H}(s) = \frac{\lambda B_{11} + B_{22}}{(1+\lambda)} - \frac{4\lambda B_{12}}{(1+\lambda)^2}$. The functions $\mathcal{L}(s)$, $\mathcal{M}(s)$, $\mathcal{G}(s)$ and $\mathcal{H}(s)$ are unchanged when λ and γ are substituted by their reciprocals λ^{-1} and γ^{-1}. The two terms on the right-hand side of (2) represent the contributions of gravity and interparticle forces to the particle relative motion, respectively. Their relative importance may be measured by the parameter $\mathcal{Q}_{\mathrm{M}} = \mu_0 M_1^2 V_1/(6\pi\mu a_1 a_2 U_{12}^{(0)})$ that can be seen as the ratio between the work done by the magnetic and the viscous forces.

4. Numerical results

The governing equations for the relative trajectories of two interacting particles were integrated by using a fourth-order Runge–Kutta scheme. The asymptotic forms of the mobility functions for widely separated spheres given were used for $s > 2.3$ [12]. Otherwise, the near-field mobilities also given by Jeffrey and Onishi [12] were implemented. In order to prevent particle overlap, we use an adaptive time step which takes into account the balance between the force acting on the particles

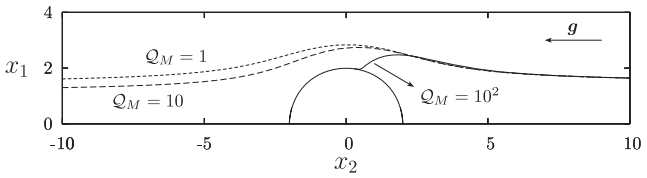

Figure 1. Relative trajectories of pairwise interacting magnetic particles. Parameter values: $\lambda = 0.5$, $\gamma = 1.0$, $x_1^{-\infty} = 1.5$, $M_{12} = 1.0$, $\hat{\boldsymbol{d}}_1 = \hat{\boldsymbol{d}}_2 = (1, 0, 0)$, $\alpha_m = 1.0$ and $Q_E = 0$.

when in close contact: the lubrication force and the magnetic force. Then, using the typical scales for the lubrication and the magnetic forces we obtain the following time step to use in the present simulations: $\delta t = \frac{1}{10}\min\{10^{-2}, \xi^2 \mathcal{Q}_{\mathrm{M}}^{-1}\}$. Applying this scheme, the errors in the numerical integration were less than 10^{-3}.

At this point we present some typical relative particle trajectories. The gravity directions are indicated in all figures by the $\boldsymbol{g}$ vector. The circle plotted with the relative trajectories represents the collision surface, whose radius is the sum of the particle radii, given by $a_1 + a_2$. Figure 1 presents results for the influence of the magnetic interaction potential $\mathcal{Q}_{\mathrm{M}}$ on the hydrodynamic diffusion process.

Figure 1 shows that for $\lambda = 0.5$, $\gamma = 1.0$, $x_1^{-\infty} = 1.5$, $M_{12} = 1.0$, $\hat{\boldsymbol{d}}_1 = \hat{\boldsymbol{d}}_2 = (1, 0, 0)$, the value $\mathcal{Q}_{\mathrm{M}} = 10$, the trajectory even though not aggregative is strongly irreversible, as can be seen by there being no null net transverse displacement, resulting a hydrodynamic diffusion process in the flow suspension of magnetic particles even for dilute regimes in which pairwise interactions dominate. In contrast, for higher values of $\mathcal{Q}_{\mathrm{M}}$ (e.g. $\mathcal{Q}_{\mathrm{M}} = 10^2$) the relative trajectory is aggregative and for small values of $\mathcal{Q}_{\mathrm{M}}$ (e.g. $\mathcal{Q}_{\mathrm{M}} = 1$) the relative trajectories are reversible.

4.1. Reversibility and irreversibility diagrams (RID)

Many phenomena can be responsible by the breaking of the relative trajectory time reversibility in Stokes flows. Among these, we note: the roughness of particles [5, 8], the particle deformation [6], the particle inertia and the presence of interparticle forces [2, 4, 14]. In this section, we are interested in the net displacement across streamlines caused by a collision. In order to represent the net streamline displacements, we plot in figure 2 the final absolute coordinates in a dimensionless form $(Y_1^{+\infty}, Y_3^{+\infty})$ for the incident sphere with initial positions $(Y_1^{-\infty}, Y_3^{-\infty})$ on a regular grid, $[0, 3.5] \times [0, 3.5]$.

The dotted lines in figures 2(a) and (b) show the limit between reversible and irreversible trajectories. This interface is defined by limit positions at which the difference between the transverse distances is given by $\Delta Y_k = |Y_k^{+\infty} - Y_k^{-\infty}| \leqslant 10^{-3}$, with $k = 1, 3$. This choice is based on a numerical error obtained in the simulations $\mathcal{O}(10^{-3})$. The depleted regions of the initial grid in figures 2(a) and (b) represent those trajectories that result in aggregation. The heterogeneous point distributions in figure 2(b) show a RID where the aggregation region and the diffusive trajectories are more evident, corresponding to the breaking of time reversibility trajectories. Furthermore, figure 2(c) represents an extreme configuration of mixing of trajectories, where the diffusive trajectories dominate. Higher values of $\mathcal{Q}_{\mathrm{M}}$ leads to a higher density of opened irreversible trajectories and a greater probability of doublet formation.

4.2. Dispersion coefficients

Although the Stokes equations are linear, the equations of particle motion are nonlinear so a tracer particle may exhibit a random walk in a suspension under the action of purely deterministic forces [10]. The interest of the present work is the case in which the hydrodynamic and magnetic interactions between the particles in a suspension are significant. This dispersive process can be characterized as a non-Brownian diffusivity which depends on the particle volume fraction ϕ and consequently on the instantaneous configuration, in contrast with ordinary Brownian suspensions.

Now, in order to obtain the hydrodynamic collective diffusivity $\boldsymbol{D}^{\mathrm{c}}(\phi)$, we consider a dispersion which has a small gradient in the concentration of m species across the streamlines, $n_j(\boldsymbol{r}) = n_j^0 + x_k(\partial n_j/\partial x_k)$, with $j = 1, \ldots, m$ and $k = 1, 3$. Following this, it is necessary to calculate the rate at which particles cross a unit area of a plane perpendicular to the concentration gradient, $x_k = 0$ for $k = 1$ or 3, due to net displacements across the streamlines. Then, we use the same procedure as was described by Cunha and Hinch [5] and,

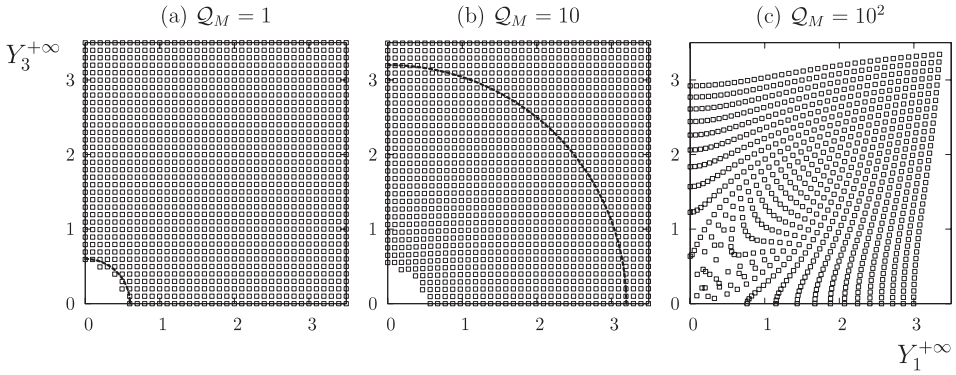

Figure 2. RID for $\lambda = 0.5$, $\gamma = 1.0$, $\hat{\boldsymbol{d}}_1 = \hat{\boldsymbol{d}}_2 = (1, 1, 0)$ and $M_{12} = 1.0$. (a) $\mathcal{Q}_{\mathrm{M}} = 1$, (b) $\mathcal{Q}_{\mathrm{M}} = 10$ and (c) $\mathcal{Q}_{\mathrm{M}} = 10^2$.

making the necessary modifications, we obtain a flux of the i species equal to

$$\mathcal{J}_i^k = \sum_{j=1}^{m} \int_{-\infty}^{\infty}\int_{-\infty}^{\infty} \left[n_i^0 n_j^0 (\Delta Y_k)_{ij} + \frac{1}{2}\left(n_j^0 \frac{\partial n_i}{\partial x_k} + n_i^0 \frac{\partial n_j}{\partial x_k} \right) \times (\Delta Y_k)_{ij}^2 + n_i^0 \frac{\partial n_i}{\partial x_k} x_k^{-\infty} (\Delta Y_k)_{ij} \right] U_{ij}\, \mathrm{d}x_1^{-\infty}\, \mathrm{d}x_3^{-\infty} \quad (3)$$

with $i, j = 1, \ldots, m$ and $k = 1$ or 3. The first term in the square bracket vanishes, as, averaging over the collisions, there is no net displacement. Hence the flux is proportional to the concentration gradient, with the coefficient of proportionality being a diffusivity. After some algebraic manipulation, equation (3) can be written as

$$\mathcal{J}_i^k = \sum_{j=1}^{m} \left\{ \int_{-\infty}^{\infty}\int_{-\infty}^{\infty} n_i^0 \left[\frac{1}{2}(\Delta Y_k)_{ij}^2 + x_k^{-\infty}(\Delta Y_k)_{ij} \right] \times U_{ij}\, \mathrm{d}S^{-\infty} + \left(\frac{n_i'}{n_j'} \right) \int_{-\infty}^{\infty}\int_{-\infty}^{\infty} n_j^0 \left[\frac{1}{2}(\Delta Y_k)_{ij}^2 \right] \times U_{ij}\, \mathrm{d}S^{-\infty} \right\} \frac{\partial n_j}{\partial x_k} = \sum_{j=1}^{m} D_{ij}^k|^{\mathrm{c}} \frac{\partial n_j}{\partial x_k}, \quad (4)$$

where $\mathrm{d}S^{-\infty} = \mathrm{d}x_1^{-\infty}\mathrm{d}x_3^{-\infty}$ and $n_i' = \partial n_i/\partial x_k$. In particular, note that the first term of equation (4) represents half the rate of change in time of the mean square displacement of the particle random walk, i.e. a self-diffusion contribution

$$D_{ij}^k|^{\mathrm{s}} = \int_{-\infty}^{\infty}\int_{-\infty}^{\infty} n_i^0 \left[\tfrac{1}{2}(\Delta Y_k)_{ij}^2 \right] U_{ij}\, \mathrm{d}S^{-\infty} \quad (5)$$

and the term

$$F_{ij}^k = \int_{-\infty}^{\infty}\int_{-\infty}^{\infty} n_i^0 \left[x_k^{-\infty}(\Delta Y_k)_{ij} \right] U_{ij}\, \mathrm{d}S^{-\infty} \quad (6)$$

is that related to the net flux produced by the concentration gradient. In a more compact form, the expression obtained in (4) can be expressed as $D_{ij}^k|^{\mathrm{c}} = D_{ij}^k|^{\mathrm{s}} + F_{ij}^k + \delta_{ij}\sum_{p=1}^{m}(n_p^0/n_i^0) D_{ip}^k|^{\mathrm{s}}$. One of the two $D_{ij}^k|^{\mathrm{s}}$ is the standard contribution of the random walk to a flux down a concentration gradient. The second one is due to the slightly higher concentration of particles colliding on one side of a test sphere systematically nudging it across the streamlines towards the lower concentration, and exists only if the two interacting particles are of the same type.

4.3. Diffusion coefficients for bidisperse dilute suspensions

Now we apply the generalized diffusion theory developed in the previous section for a bidisperse dilute suspension. From equation (4), one can write the expressions for the flux of particles 1 and 2 in the x direction (transverse to gravity) as being $\mathcal{J}_1 = D_{11}|^{\mathrm{c}}(\partial n_1/\partial x) + D_{12}|^{\mathrm{c}}(\partial n_2/\partial x)$ and $\mathcal{J}_2 = D_{21}|^{\mathrm{c}}(\partial n_1/\partial x) + D_{22}|^{\mathrm{c}}(\partial n_2/\partial x)$, where the collective dispersion coefficients $D_{ij}|^{\mathrm{c}}$ are given by $D_{11}|^{\mathrm{c}} = 2D_{11}|^{\mathrm{s}} + F_{11} + (n_2^0/n_1^0)D_{12}|^{\mathrm{s}}$; $D_{12}|^{\mathrm{c}} = D_{12}|^{\mathrm{s}} + F_{12}$; $D_{21}|^{\mathrm{c}} = D_{21}|^{\mathrm{s}} + F_{21}$; $D_{22}|^{\mathrm{c}} = 2D_{22}|^{\mathrm{s}} + F_{22} + (n_1^0/n_2^0)D_{21}|^{\mathrm{s}}$. These expressions make explicit the additional self-diffusion terms that are related to non-uniform concentration of particles colliding on one side of a test particle. In particular, for sedimenting suspensions, the terms $D_{11}|^{\mathrm{s}}$, F_{11}, $D_{22}|^{\mathrm{s}}$ and F_{22} are all null. Then, it is necessary to evaluate the diffusivities $D_{12}|^{\mathrm{c}}$ and $D_{21}|^{\mathrm{c}}$.

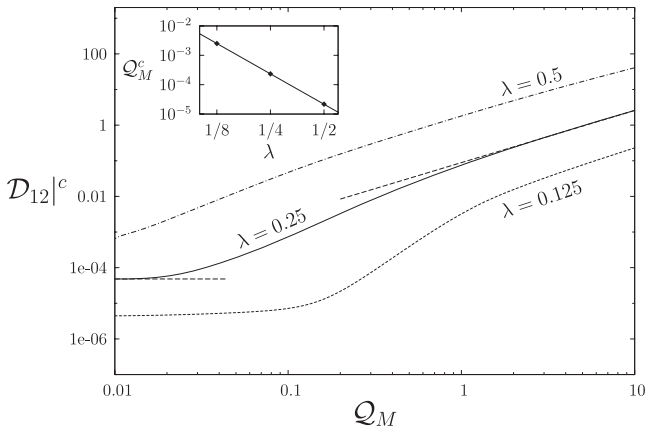

Figure 3. Dimensionless down-gradient dispersion coefficient of the incident particle 1 in a suspension of magnetic particles for $\gamma = 1.0$, $M_{12} = 0.8$, and $\hat{\boldsymbol{d}}_1 = \hat{\boldsymbol{d}}_2 = (1, 1, 1)$.

Now, making dimensionless the lengths of the integrand of (5) and (6) using the effective radius $\bar{a} = (a_1 + a_2)/2$ one may write the diffusion coefficients in a dimensionless form. For instance, we have the following dimensionless expressions for $D_{12}|^{\mathrm{s}}$ and F_{12}:

$$\mathcal{D}_{12}|^{\mathrm{s}} = \frac{D_{12}|^{\mathrm{s}}}{U_{12}^{(0)}\bar{a}\phi_1^0} = \int_{-\infty}^{\infty}\int_{-\infty}^{\infty} \left[\frac{3}{8\pi}\left(\frac{1+\lambda}{2} \right)^3 (\Delta Y)_{12}^2 \right] \mathrm{d}S^{-\infty} \quad (7)$$

and

$$\mathcal{F}_{12} = \frac{F_{12}}{U_{12}^{(0)}\bar{a}\phi_1^0} = \int_{-\infty}^{\infty}\int_{-\infty}^{\infty} \left[\frac{3}{4\pi}\left(\frac{1+\lambda}{2} \right)^3 x_k^{-\infty}(\Delta Y_k)_{ij} \right] \mathrm{d}S^{-\infty}. \quad (8)$$

Figure 3 presents results for the down-gradient diffusivity coefficient $\mathcal{D}_{12}|^{\mathrm{c}}$ of the incident particle, for different values of the polydispersity parameter λ. For $\gamma = 1.0$, $M_{12} = 0.8$, and $\hat{\boldsymbol{d}}_1 = \hat{\boldsymbol{d}}_2 = (1, 1, 1)$, it is seen that higher values of λ lead to a higher diffusion coefficient. This is a direct consequence of the increasing effect of gravity compared to the interparticle magnetic force for lower values of λ. Then, as the dispersion is produced due to an intrinsic source of irreversibility of the suspension (in the present case, the magnetic interaction), for $\lambda = 0.5$ the down-gradient diffusivity is about 20 times greater than the one obtained for $\lambda = 0.25$. In the same plot it is shown that for the case in which $\lambda \ll 1$ (e.g. $\lambda = 0.25$) and $\mathcal{Q}_{\mathrm{M}} \ll 1$ the coefficient $\mathcal{D}_{12}|^{\mathrm{c}}$ tends to 4.7×10^{-5}. Smaller values of λ require a minimum value of $\mathcal{Q}_{\mathrm{M}}^{\mathrm{c}}$ (critical value) in order to produce a substantial change on $\mathcal{D}_{12}|^{\mathrm{c}}$. The inset in figure 3 shows the dependence of $\mathcal{Q}_{\mathrm{M}}^{\mathrm{c}}$ on λ. The results reveal a power-law behaviour with $\mathcal{Q}_{\mathrm{M}}^{\mathrm{c}} \cong (2 \times 10^{-6})\lambda^{-17/5}$.

Besides, for $\mathcal{Q}_{\mathrm{M}} \gg 1$, it is seen clearly that the diffusion coefficient $\mathcal{D}_{12}|^{\mathrm{c}}$ has a power-law behaviour. We also plot

this asymptotic limit for $\lambda = 0.25$, obtaining the expression $\mathcal{D}_{12}|^{c} \cong (9/100)\mathcal{Q}_{M}^{3/2}$. The power of $\mathcal{Q}_{M}$ in the expression of $\mathcal{D}_{12}|^{c}$ is independent of the polydispersity parameter, so for all λ we propose a more generalized formula for this asymptotic limit as $\mathcal{D}_{12}|^{c} \cong c_0(\lambda)\mathcal{Q}_{M}^{3/2}$, the same for the conditions $\lambda = 0.5$ and 0.125. In addition, figure 3 presents the magnitude of the dispersion effect produced by the two-particle magnetic interaction in comparison with the calculations based on breaking the symmetry of the particle trajectory examined by Davis [8]. We can see that the maximum value of the lateral diffusivity coefficient obtained for rough particles [8] is about 70 times lower than that obtained for the case $\lambda = 0.5$ and $\mathcal{Q}_{M} = 10^2$, which indicates a significant influence of the magnetic dipole–dipole interaction on the hydrodynamic diffusive process investigated.

5. Conclusions

The dispersive process examined here was not produced by Brownian motion since the particle diffusivity depends on the particle volume fraction of the suspension. A key dimensionless parameter has been identified, denoted by $\mathcal{Q}_{M}$, which provides a measure of the relative importance of work done by the magnetic force and that done by the viscous force. The down-gradient diffusivity of a magnetic test sphere having volume fraction ϕ in a bidisperse suspension has been computed, giving $D = c(\lambda)U_{12}^{0}\bar{a}\phi\mathcal{Q}_{M}^{3/2}$. Our results have indicated a significant influence of the magnetic dipole–dipole pairwise interactions on the hydrodynamic diffusion of micromagnetic composites during sedimentation.

Acknowledgments

The authors acknowledge the financial support given by CAPES, CNPq and FINATEC.

References

[1] Eckstein E C, Bailey D G and Shapiro A H 1977 *J. Fluid Mech.* **79** 191
[2] Adler P M 1981 *J. Colloid Interface Sci.* **83** 461
[3] Wang Y, Mauri R and Acrivos A 1996 *J. Fluid Mech.* **327** 255
[4] Wang Y, Mauri R and Acrivos A 1998 *J. Fluid Mech.* **357** 279
[5] Cunha F R and Hinch E J 1996 *J. Fluid Mech.* **309** 211
[6] Loewenberg M and Hinch E J 1997 *J. Fluid Mech.* **338** 299
[7] Davis R H and Hill N A 1992 *J. Fluid Mech.* **236** 513
[8] Davis R H 1992 *Phys. Fluids* A **4** 2607
[9] Sierou A and Brady J F 2004 *J. Fluid Mech.* **506** 285
[10] Leshansky A M and Brady J F 2005 *J. Fluid Mech.* **527** 141
[11] Kim S and Karrila S J 2005 *Microhydrodynamics* (New York: Dover)
[12] Jeffrey D J and Onishi Y 1984 *J. Fluid Mech.* **139** 261
[13] Rosensweig R E 1985 *Ferrohydrodynamics* (New York: Dover)
[14] Melis S, Verduyn M, Storti G, Morbidelli M and Baldyga J 1999 *AIChE J.* **45** 1383